

**2. Phytoplankton and Optical Oceanography; submitted by Christopher D. Hewes (Legs I & II), John Wieland (Leg II), B. Greg Mitchell (SIO), Mati Kahru (SIO), and Osmund Holm-Hansen (SIO).**

**2.1 Objectives:** The overall objective of our research project was to assess the distribution and concentration of food reservoirs available to the herbivorous zooplankton populations throughout the AMLR study area during the austral summer. Specific objectives of our work included: (1) to determine the distribution and biomass of phytoplankton in the upper water column (surface to 200m), with emphasis on the upper 100m; (2) to measure pigment-specific absorption by total particulates, detritus and phytoplankton; (3) to measure the spectral attenuation of light with depth; (4) to coordinate these activities with SeaWiFS satellite coverage; (5) to calibrate satellite imagery of spectral reflectance to surface chlorophyll concentrations.

**2.2 Methods and Accomplishments:** The major types of data acquired during these studies, together with an explanation of the methodology employed, are listed below.

**(A) Sampling Strategy:**

Protocols were to both obtain water samples for analyses and to acquire data from various sensors:

(1) During Leg I, water samples were obtained from 10-liter Niskin bottles (with Teflon covered springs) which were closed at 5 meters for every station plus eight other standard depths (10, 20, 30, 40, 50, 75, 100, and 200m) from every other station upcast of the CTD/rosette unit. During Leg II, 5m samples were obtained using 10-liter Niskin bottles at all stations plus at eight standard depths (as above) for those stations where optical profiles were also made (minimum of one per day).

(2) During Leg I, one transmissometer (660nm wavelength), and for Leg II, two transmissometers (488 and 660nm wavelengths) were used to determine the attenuation of collimated light (by both scattering and absorption) during CTD-casts.

(3) For both legs, a profiling *in situ* fluorometer was used to measure chlorophyll fluorescence.

(4) A solar irradiance sensor (BSI Inc. model QCP-200L) with a cosine response was used for recording of attenuation of photosynthetically available radiation (PAR) with depth during both legs.

(5) For both legs, SeaWiFS satellite images were processed for monthly averaged chlorophyll concentrations.

**(B) Measurements and Data Acquired:**

(1) Chlorophyll-*a* concentrations: Chl-*a* concentrations in the water samples were determined by measurement of chl-*a* fluorescence after extraction in an organic solvent. Sample volumes of 100ml were filtered through glass fiber filters (Whatman GF/F, 25mm) at reduced pressure

(maximal differential pressure of  $1/3^{\text{rd}}$  atmosphere). The filters with the particulate material were placed in 10ml of absolute methanol in 15ml tubes and the photosynthetic pigments allowed to extract at 4EC for at least 12 hours. The samples were then shaken, centrifuged, and the clear supernatant poured into cuvettes (13 x 100mm) for measurement of chl-*a* fluorescence before and after the addition of two drops of 1.0 N HCl. Fluorescence was measured using Turner Designs Fluorometer model #700 having been calibrated using spectrophotometrically determined chl-*a* concentrations of a prepared standard (Sigma). Stability of the fluorometer was verified daily by using a fluorescence standard.

(2) Miscellaneous optical and cellular measurements: For 33 stations during Leg II, discrete water samples were obtained between 1000 and 1600 GMT (corresponding with the time that SeaWiFS satellite observations of the area became available) for pigment analyses. Water bottle samples obtained at six discrete depths were used for each of the following analyses (except where noted 1-2 liters were filtered through 25mm Whatman GF/F filters).

- Particulate Absorption ( $a_p$ ) and Soluble Absorption ( $a_s$ ). Spectral absorption coefficients of particulate and soluble material were performed on a CARY 100 dual beam spectrophotometer.
- High Pressure Liquid Chromatography (HPLC). HPLC will be used for the analysis of (1) various chlorophylls and associated pigments, and (2) Microsporine-like Amino Acids (MAAs). Samples were frozen and stored in liquid nitrogen until their analyses can be made at SIO. Chlorophyll and associated pigments will be used to determine the proportions of algal classes contained in the phytoplankton community. MAAs absorb ultraviolet-B radiation and are thought to protect phytoplankton against photo-oxidative damage of cellular components by UV damage to the photosystem.
- Particulate Organic Carbon and Nitrogen (POC and PON). Whatman GF/F filters used for sample preparation were combusted at 450EC prior to the cruise. Samples were frozen and will be analyzed by standard gas chromatography methods at the analytical facility at the University of California at Santa Barbara.
- Phycoerythrins (PE). Cryptomonads are a common phytoflagellate in the AMLR study region and are distinguished from other phytoplankton in the area by PE. The filtered water samples were frozen and stored in liquid nitrogen until their analysis at SIO. PE will be measured using a Spex Fluoromax spectrofluorometer.
- Cell size spectrum. Two ml of water were frozen and stored in liquid nitrogen until analysis. A Coulter Epics flow-cytometer will be used to size cells and classify them in relation to chlorophyll and phycoerythrin fluorescence as well as forward light scatter.

(3) Measurement of beam attenuation: During Leg I, a single (660nm) and during Leg II, two single wavelength (488 and 660nm) C-star transmissometers (Wetlabs, Inc.) were placed on the Seabird Inc. CTD rosette for deployment at each station. Previous studies have shown that beam attenuation (660nm) coefficients can be used to estimate total particulate organic carbon in Antarctic waters (Villafañe *et al.*, 1993). This calculation assumes that there is a negligible load

of inorganic sediment in the water, a condition that is apparently satisfied throughout the study area.

(4) *In situ* optical oceanography: Corresponding approximately in time with the optimal time that the SeaWiFS satellite passed over (31 stations), a Biospherical Instruments free-fall Profiling Reflectance Radiometer (PRR-800) was deployed. The PRR-800 measured spectral downwelling ( $E_d$ ) and upwelling ( $E_u$ ) irradiances and upwelling radiance ( $I_u$ ) at 19 wavelengths continuously from the surface to the bottom of the profile. Profile depths ranged from 50-200 meters depending on the station. Spectral values of normalized water-leaving radiance will be computed from the PRR-800 data and used to validate SeaWiFS data, as well as to develop Southern Ocean regional ocean color algorithms.

(5) Satellite Oceanography: SeaWiFS chlorophyll images were obtained for 8-day and monthly average composites from NASA archives. These data will be sufficient to evaluate the time-dependence and distribution of chl-*a* within our study region.

## **2.3 Results and Tentative Conclusions:**

### **(A) Phytoplankton Biomass**

**Leg I** (Refer to Figure 2.1A). In the Bransfield Strait south of the South Shetland Islands (South area), mild phytoplankton blooming was found having average chlorophyll concentrations of  $1.8\text{mg m}^{-3}$  at 5-meter depth and approximately  $73\text{mg m}^{-2}$  as integrated through the water column to 100 meters. The pattern for surface chlorophyll concentrations in the Elephant Island sector closely followed bottom topography of the area. Although 5m chlorophyll averages  $0.62 \pm 0.64\text{mg m}^{-3}$  for the entire section, the shelf and break area around Elephant Island (29 stations) averaged  $1.01 \pm 0.67\text{mg chlorophyll m}^{-3}$  as compared to  $0.26 \pm 0.28\text{mg chlorophyll m}^{-3}$  in the oceanic region. The pattern for surface chlorophyll concentrations in the West Area closely followed bottom topography similar to the Elephant Island Area. Five-meter chlorophyll was  $0.71 \pm 10\text{ mg m}^{-3}$  for the entire section (29 stations) with stations located in waters less than 1,000-meter depth having  $2.7 \pm 0.49\text{mg chlorophyll m}^{-3}$  as compared with pelagic stations having  $0.18 \pm 0.21\text{mg chlorophyll m}^{-3}$ .

The southwestern portion of the Bransfield Strait (Stations A180, A190, and A191) had the highest 5m chlorophyll concentrations of Leg I, having  $3.36 \pm 0.26\text{mg m}^{-3}$ . However, these concentrations were greatly attenuated to less than  $1.2\text{mg m}^{-3}$  by 20- to 30-meter depth thus contributing less integrated biomass than those stations lying along the shelf region north of the South Shetland Islands. The second most phytoplankton rich area measured during Leg I was found within the continental shelf north of the South Shetland Islands with stations A150 and A174 having greater than  $2.5\text{mg chlorophyll m}^{-3}$ .

**Leg II** (Refer to Figure 2.1B). The pattern for surface chlorophyll concentrations in the West Area closely followed bottom topography similar to that observed during Leg I. Five-meter chlorophyll was  $0.37 \pm 0.44\text{mg m}^{-3}$  for the entire section (29 stations) with stations located in waters less than 1,000-meter depth having  $1.06 \pm 0.49\text{mg chlorophyll m}^{-3}$  as compared with pelagic stations having  $0.18 \pm 0.17\text{mg chlorophyll m}^{-3}$ . Thus, mean near-surface chlorophyll in

continental and shelf breakwaters declined by more than 50% since Leg I, while values for the Drake Passage waters remained near the same. During Leg I, stations A150 and A174 were among the richest of the survey having greater than 2.5mg chlorophyll m<sup>-3</sup> each, however station D150 had decreased to 2.0mg chlorophyll m<sup>-3</sup> and station D174 decreased down to 1.1mg chlorophyll m<sup>-3</sup> during Leg II.

The pattern for surface chlorophyll concentrations in the Elephant Island Area closely followed bottom topography similar to that observed during Leg I. However, 5m chlorophyll was  $0.40 \pm 0.34\text{mg m}^{-3}$  for the entire section (46 stations) with stations located in waters less than 1,000-meter depth having  $0.66 \pm 0.34\text{mg chlorophyll m}^{-3}$  (15 stations) as compared with pelagic stations having  $0.28 \pm 0.27\text{mg chlorophyll m}^{-3}$ . Thus, mean near-surface chlorophyll declined about 40% since Leg I ( $0.62 \pm 0.64\text{mg m}^{-3}$  for the entire section,  $1.01 \pm 0.67$  and  $0.26 \pm 0.28\text{mg chlorophyll m}^{-3}$  in the shallow and oceanic region regions, respectively).

The general pattern of phytoplankton biomass as observed over the past 10 seasons indicate that chlorophyll concentrations generally increase during Leg II compared to Leg I for the AMLR region. This year Leg I chlorophyll concentrations (Figure 2.1A) decreased during Leg II (Figure 2.1B). However, this will be discussed further in context to satellite observations (See 2.B.1 below). Compared with previous years (1990-1999), chlorophyll concentrations for the South Area were slightly higher this year than the average of about 1.2mg m<sup>-3</sup> (note however the fewer number of stations), and slightly less this year for the West and Elephant Island Areas (about 0.8 -1.0mg m<sup>-3</sup>, respectively) at 5m.

## **(B) Satellite/Optical Oceanography**

The optical oceanography component incorporated to the program (funded by NASA's SIMBIOS program to Dr. Greg Mitchell, SIO), provided satellite (SeaWiFS) images of surface chlorophyll distributions, as well as *in-situ* optical profiling and pigment spectrophotometry during Leg II.

1. Monthly composite chlorophyll distributions from SeaWiFS images for January and February for the AMLR survey region (Figure 2.2A, C) support the observation that directly measured chlorophyll concentrations declined between January and February. Some of this may be reconciled by placing this in perspective of the entire Scotia Sea (Figures 2.2B, D). A belt of blue water (Water Zone 1A) lies between South America and the Antarctic Peninsula, and high chlorophyll concentrations appear to reach from the Bransfield Strait region to South Georgia. Also note how high chlorophyll concentrations follow the contours of the shelves for South America and the South Shetland Islands (Figures 2.2B, D), but greatest blooming occurred in the central Scotia Sea between the shallower depths of the entire Scotia Ridge. In addition, it is evident that the summer bloom that has been noted to occur in February did so, but apparently slightly northeastward of our survey area. A bloom also developed at the southwestern portion of the Bransfield Strait during February (Figure 2.2C), but we had too few stations in the region to have determined this from extracted chlorophyll measurements.

2. One of the key parameters obtainable from satellite measurements is the spectral reflectance, or ocean color, which contains information about optically significant constituents of seawater.

The AMLR survey region is a complex system with significant internal gradients in forcing and biogeochemical properties. The bio-optical properties for bio-geographic provinces of this region and their relation to photosynthesis, biomass, carbon and production are currently being studied. An example of this can be obtained from examination of two contrasting stations from Leg II, D166 (a Drake Passage water type, Figures 2.3A, B) and D014 (a coastal station, Figures 2.3C, D). Drake Passage water (Zone IA waters) is characteristic of having low chlorophyll biomass ( $> 0.5\text{mg chlorophyll m}^{-3}$ ) in the upper 100 meters, but a small chlorophyll maximum found between 50 and 120 meters (Figure 2.3B; corresponding with the depth of a water temperature minimum). This is in contrast with more productive coastal waters where phytoplankton biomass is located in the upper portion of the euphotic zone. It is well known that phytoplankton account for most of the particulate absorption of light and hence attenuation of photosynthetically available irradiation (PAR) in the water column. Therefore, PAR is attenuated more rapidly with depth in the water column at a rich coastal station (Figure 2.3C) as compared to that of a blue water station (Figure 2.3A).

The spectral irradiance in the ocean is complex and varies considerably depending upon its environment (i.e., clarity, depth, particulates, and incidental sunlight). Apparent optical properties of water including the diffuse attenuation coefficient (K) that specifies the rate of light attenuation of the ocean and the reflectance (R), which is the "ocean color", depend on inherent optical properties (absorption and scattering) of the medium. Water may contain variable amounts of particulates or soluble material, which affect inherent and apparent optical properties (Morel and Prieur, 1977; Smith and Baker, 1978; Morel, 1988; Mitchell and Holm-Hansen, 1991; Arrigo *et al.*, 1998). Phytoplankton are the most dominant particles having color in the oceans, and contain various photosynthetic and non-photosynthetic pigments (Figure 2.4). R and K have been shown to correlate well with the phytoplankton pigments biomass (e.g. chl-*a*) because absorption by pigments dominates variability in these properties. Water color (Figure 2.5) therefore greatly depends not only on both the taxonomic family of phytoplankton present (which determines the types of pigments present), but also on their concentration with depth. As a result, the quality and quantity of light upwelled from the oceans surface is dependent upon the absorption and scattering qualities of the phytoplankton present. As expected, the upwelling radiance normal to incident irradiance of a blue water station (Figure 2.5A; Station D166) is greater and of different color (note the "blue" spectral peak) than that of the richer station (Figure 2.5B; Station D014) that has a greater "green" spectral component.

It is noted that the absorption spectrum of phytoplankton (Figure 2.4) provides two major peaks (about 440 and 670nm) that are ascribed to chlorophyll, plus a variety of shoulders in the spectra that represent additional pigmentation. Furthermore, there is a general absence of absorption in the green (550-600nm) wavelengths. When the proportions of upwelled light at 443 to 555nm are examined (Figure 2.5 & 2.6), a great contrast can be measured between "blue-water" (e.g., D166) and "green-water" (e.g., D014). The ratio of 443:555nm upwelled radiance is a function of chlorophyll concentration and this relationship changes with depth (Figure 2.6). Thus, the ratio of 443:555nm upwelled radiance at the ocean surface can be obtained by SeaWiFS satellite, and was a first approximation for the estimation of chlorophyll from space (see O'Reilly *et al.*, 1998). The most recent of algorithms for estimation of chlorophyll concentration also use the 443 and 555nm channels, so that data plotted in Figure 2.7 are relevant: SeaWiFS algorithms used to estimate chlorophyll (and primary productivity) must necessarily be different for the

Southern Ocean (represented by the AMLR data) than that estimated for mid-latitudes (represented by the CalCOFI data in Figure 2.7). It is apparent from the data presented in Figure 2.7 that surface chlorophyll estimates for the AMLR study areas and associated Antarctic regions may be underestimated greatly if general SeaWiFS algorithms are used, and this supports previous predictions (Mitchell, 1992; Moore, 1999).

**2.4 Disposition of the Samples and Data:** All data obtained during the cruises have been stored on CD-ROM. After compilation of the final data sets, a copy of all data will be deposited with Dr. Roger Hewitt in the AERD office in La Jolla, CA. Copies of any of our data sets are available to all other AMLR investigators upon request.

**2.5 Problems and Suggestions:** It should be noted that NOAA funding for the AMLR program does not provide funds for the calibration, repair, or replacement of field equipment (both laboratory equipment and *in situ* sensors) used in the annual surveys. Many of our instruments devoted to this program (originally obtained from other funding agencies) for the past 12 years are now beginning to fail. Unless some additional NOAA funding can be found to replace such instruments, the scope and quality of our data in future AMLR field years will be compromised.

**2.6 Acknowledgements:** We want to express our gratitude and appreciation to the entire complement of the R/V *Yuzhmorgeologiya* for their generous and valuable help during the entire cruise. They not only aided immeasurably in our ability to obtain the desired oceanographic data, but they also made the cruise most enjoyable and rewarding in many ways. We also thank all other AMLR personnel for help and support which was essential to the success of our program. This paper is funded in part by a grant from the National Oceanic and Atmospheric Administration, U.S. Department of Commerce, under grant NA77RJ0453, and by NASA SIMBIOS Project awards to B. Greg Mitchell (NAS5-97130 and NAS5-01002). The views expressed herein are those of the authors and do not necessarily reflect the views of NOAA or any of its sub-agencies.

## 2.7 References:

- Arrigo, K.R., Robinson, D.H., Worthen, D.L., Schieber, B., and Lizotte. 1998. Bio-optical properties of the southwestern Ross Sea. *Journal of Geophysical Research* 103 (C10): 21683-21695.
- Mitchell, B.G., and Holm-Hansen, O. 1991. Bio-optical properties of Antarctic Peninsula waters: differentiation from temperate ocean models. *Deep-Sea Research I* 38 (8/9): 1009-1028.
- Mitchell, B.G. 1992. Predictive bio-optical relationships for polar oceans and marginal ice zones. *Journal of Marine Systems* 3: 91-105.
- Moore, J.K., Abbott, M.R., Richman, J.G., Smith, W.O., Cowles, J.R., Coale, K.H., Gardner, W.D., and Barber, R.T. 1999. SeaWiFS satellite ocean color data from the Southern Ocean. *Geophysical Research Letters* 26(10): 1465-1468.
- Morel, A. 1988. Optical modeling of the upper ocean in relation to its biogenous matter content (case I waters). *Journal of Geophysical Research* 93(C9): 10749-10768.
- Morel, A., and Prieur, L. 1977. Analysis of variations in ocean color. *Limnology and Oceanography* 22: 709-722.
- Smith, R.C., and Baker, K.S. 1978. The bio-optical state of ocean waters and remote sensing. *Limnology and Oceanography* 23: 247-259.
- Villafañe, V., Helbling, E.W., and Holm-Hansen, O. 1993. Phytoplankton around Elephant Island, Antarctica: distribution, biomass and composition. *Polar Biology* 13: 183-191.

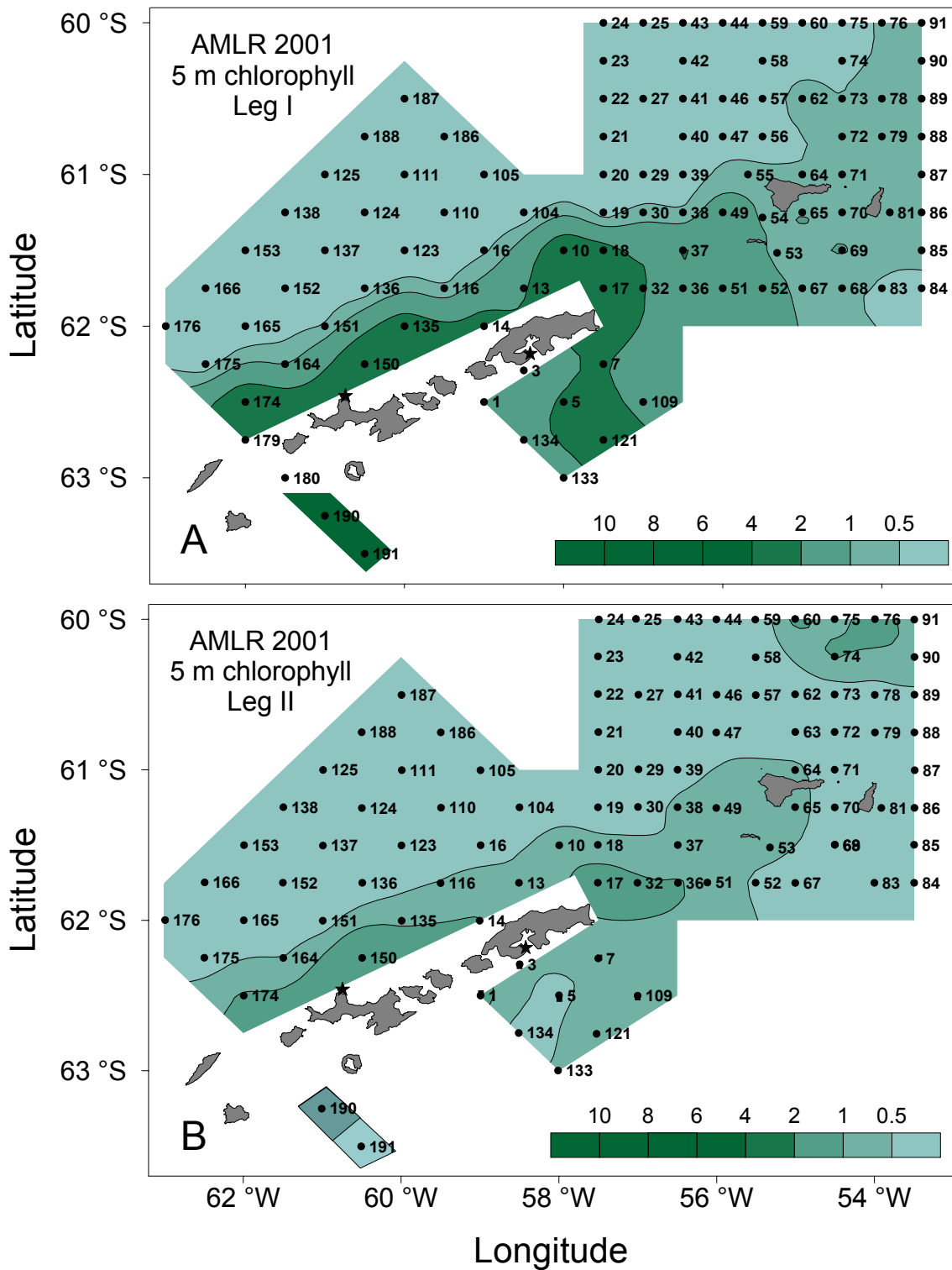


Figure 2.1. Distribution of chl-*a* concentration as obtained from Niskin bottle for stations during Leg I (A) and Leg II (B). Note 1) the elevated concentrations aligned with the island groups that corresponds with the shelf and break region of the South Shetland Islands, and 2) the general decrease of chlorophyll concentration from Leg I to Leg II.



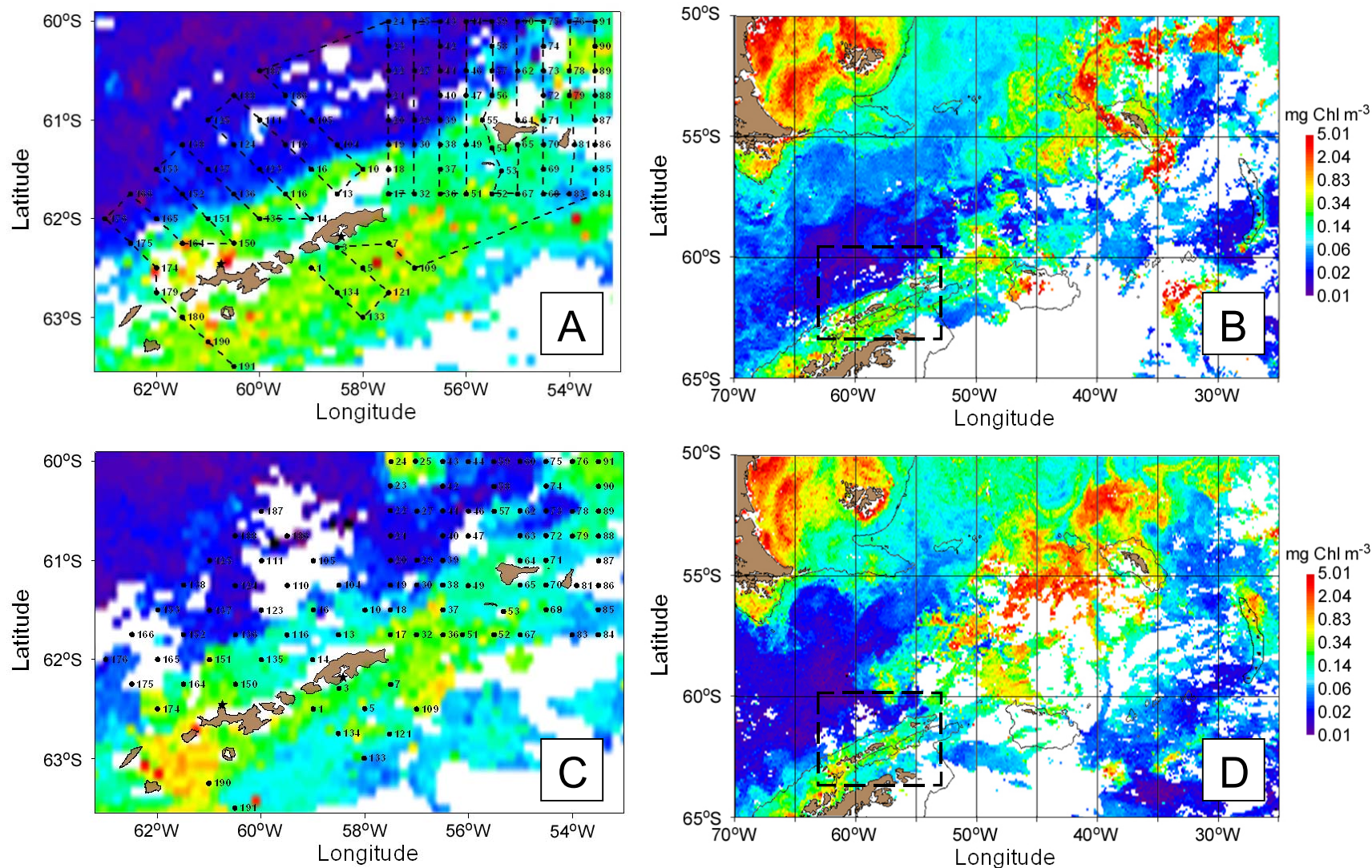


Figure 2.2. SeaWiFS satellite derived monthly composite chlorophyll concentrations for January (A, B) and February (C, D) for the AMLR survey area (A, C) and the entire Scotia Sea (B, D). Portion of the Scotia Sea area that the U.S. AMLR program surveys is indicated by a box in B and D. Although chl-*a* concentrations decreased in the AMLR survey region from January (A) through February (C), this was apparently a local phenomena, since much of the Scotia Sea developed blooms between January (B) and February (D).

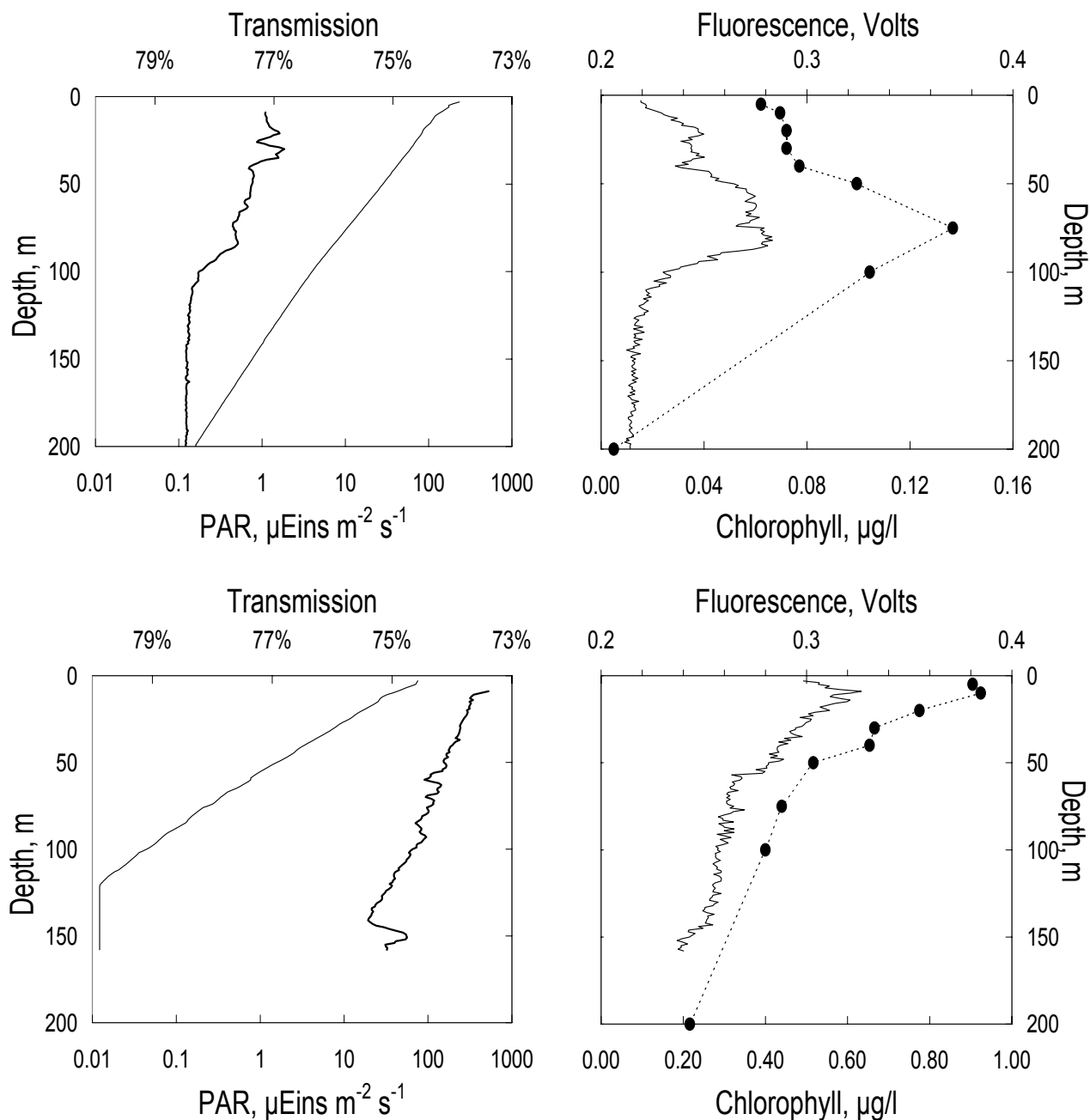


Figure 2.3. Optical and biological measures comparing a blue water Station D166 (A, B) and green water Station D014 (C, D) from Leg II (refer to Figure 2.1B & 2.2C for station references). Percent transmission (thick line) is much greater at D166 (A) than D014 (C) primarily as a function of chl-*a* concentration (symbols with dotted line) which was much less for D166 (B) than D014 (D). *In vivo* fluorescence (thin line) followed profiles of chlorophyll concentrations for both stations (B, D). Incident photosynthetically available radiation (PAR, thin line) was attenuated more rapidly with depth as a function of chlorophyll concentration in the green water station (C) than for the blue water station (A).

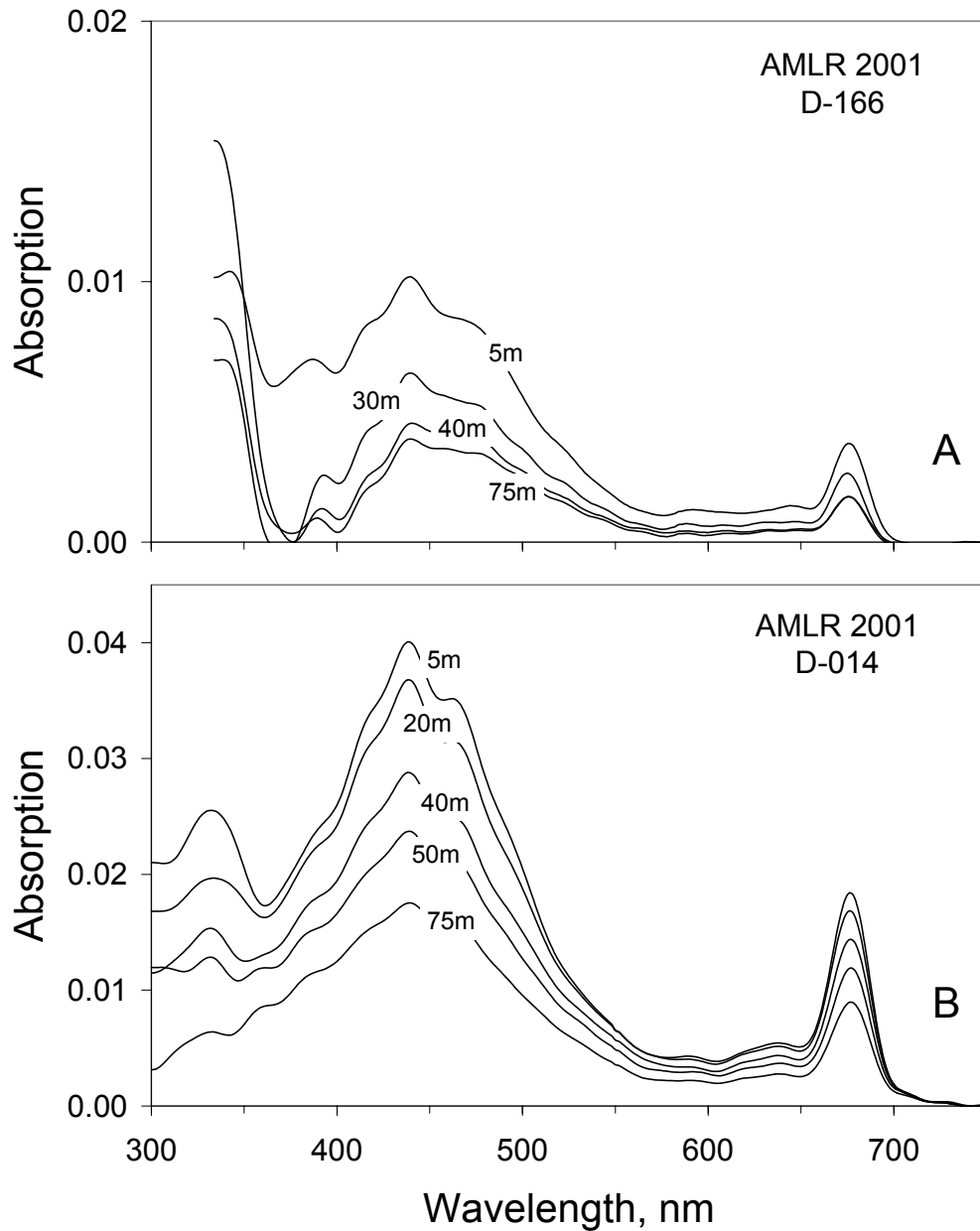


Figure 2.4. Spectral qualities of the phytoplankton populations sampled at different water depths for a blue water station, D166 (A) and a green water station, D014 (B). The scattering and attenuation of incident light in the water column (refer to Figure 2.3) is primarily a function of phytoplankton that contain various photosynthetic and non-photosynthetic pigments. Absorption by phytoplankton is dependent upon both their biomass and the taxonomy of phytoplankton, which determine the types and concentrations of other pigments in addition to chlorophyll that are present.

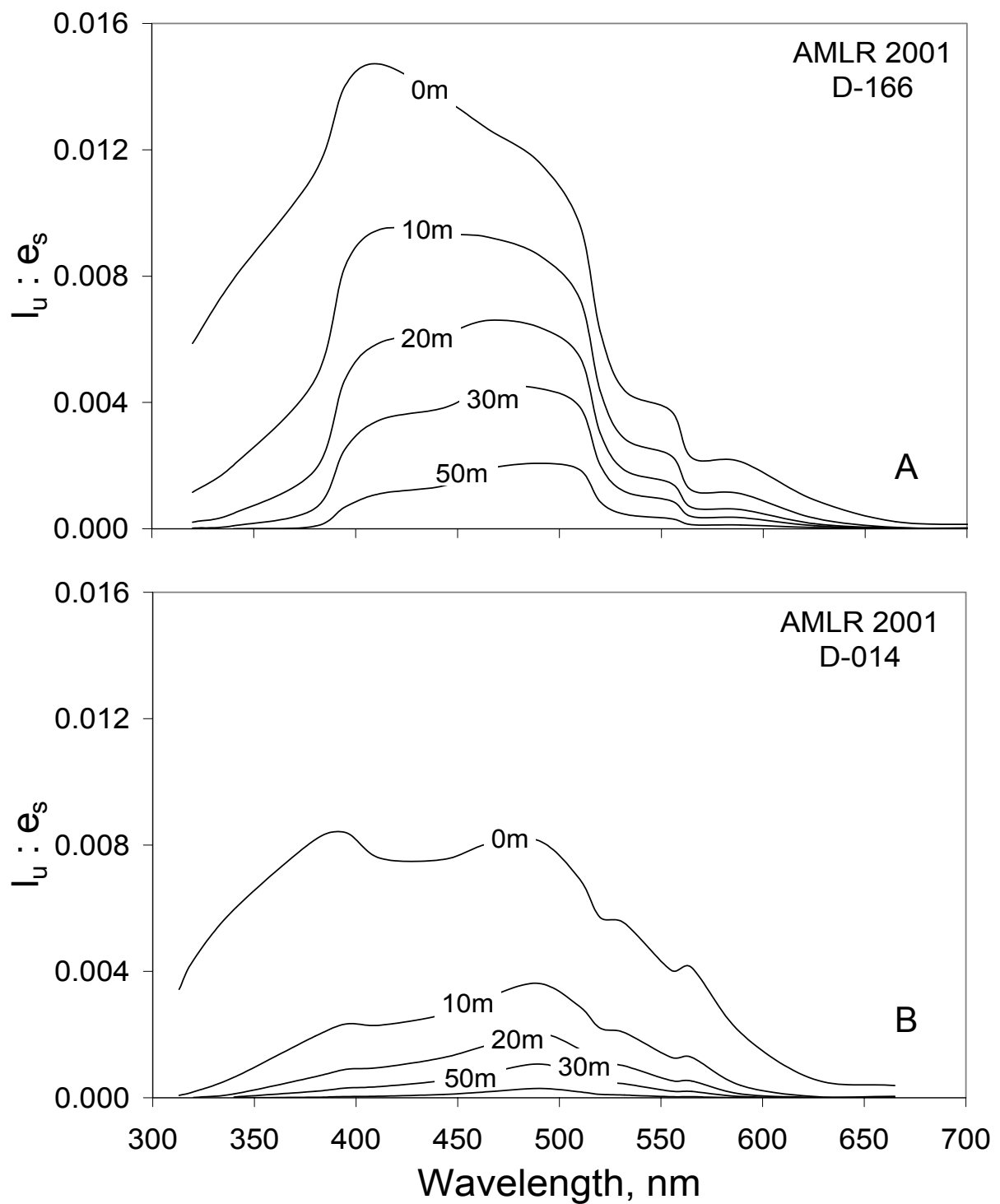


Figure 2.5. The types of pigments and their concentrations in the phytoplankton population determine the relative spectra of upwelled light ( $I_u$ ) relative to incident radiation ( $e_s$ ). Therefore it is seen that the blue water station D166 (A) had relatively higher amounts of upwelled blue light at the surface than did the green water station D014 (B), since it had less concentrations of chlorophyll and other "blue" absorbing pigments as shown by their spectra in Figure 2.4.

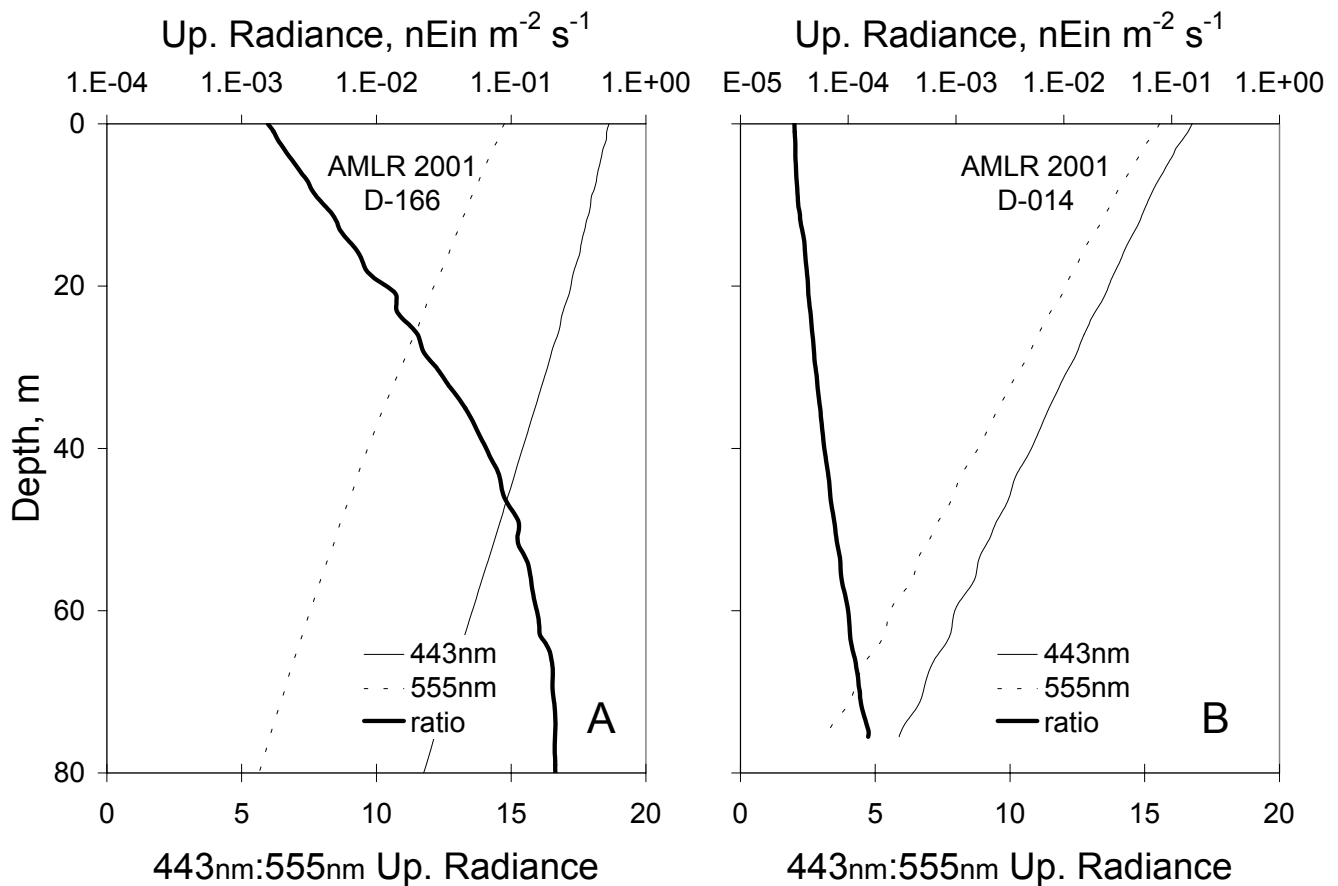


Figure 2.6. The upwelled radiance (a function of particle scattering) measured at depth (thin lines) is attenuated faster for green water than for blue water because downwelled PAR from the surface is attenuated at a greater rate (Figure 2.3A, C). Blue light penetrates further into the water column than green or red light, however *in vivo* chl-*a* absorbs light at about 443nm, while phytoplankton in general have little absorption of light at 555nm (refer to Figure 2.4). Therefore blue water (A, Station D166) will have greater upwelled light at 443nm (thin solid line) and 555nm (thick solid line) than for a rich station (B, Station D014) because there is a greater amount of PAR at depth. However, even though 443nm light penetrates a water column further, it is absorbed by chlorophyll, thus changing the ratio (thick line) of blue:green wavelengths in the richer station (B, D014) compared with a low biomass station (A, A166). The result is that a "blue" water station looks blue because it has more upwelled radiance in the blue wavelengths than a chlorophyll rich station.

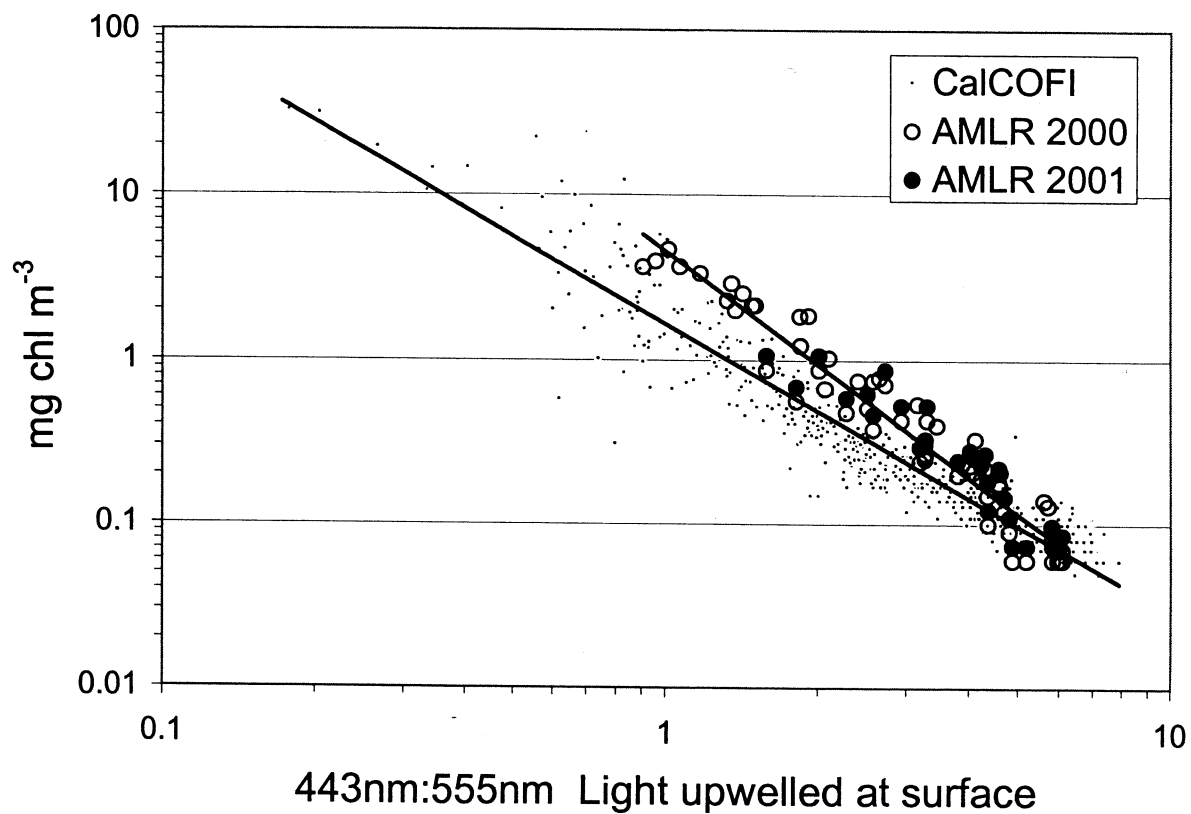


Figure 2.7. The ratio of 443nm to 555nm radiance upwelled at the surface is proportional to the concentration of chlorophyll in the first few meters of the water column. However, samples from the AMLR surveys demonstrate a higher 443:555nm value per unit chlorophyll than samples taken from Californian (CalCOFI) waters and emphasize that algorithms developed to estimate concentrations remotely either from shipboard or satellite need be made specifically for individual regions.